Histol Histopathol (2020) 35: 203-216

http://www.hh.um.es

Histology and Histopathology

From Cell Biology to Tissue Engineering

Comparative study of calcium and calcium-related enzymes with differentiation markers in different ages and muscle types in *mdx* mice

Rhayanna B. Gaglianone[1,2], Flavia Fonseca Bloise[3], Tania Maria Ortiga-Carvalho[3], Thereza Quirico-Santos[2], Manoel Luis Costa[1] and Claudia Mermelstein[1]

[1]Biomedical Sciences Institute, Federal University of Rio de Janeiro, [2]Biology Institute, Fluminense Federal University, Niterói and [3]Carlos Chagas Filho Biophysical Institute, Federal University of Rio de Janeiro, Rio de Janeiro, RJ, Brazil

Summary. Sarcolemma instability and increased calcium influx in muscle fibers are characteristics of the Duchenne muscular dystrophy. Excessive calcium activates calcium-dependent enzymes, such as calpains (CAPN) and matrix metalloproteases (MMP). Here, we analyzed calcium deposits, the activity of CAPN and MMP and the expression of *Myh*, SERCA and myogenic regulatory factors in different skeletal muscles during myonecrosis (4-weeks) and regeneration (12-weeks) phases of the *mdx* muscular pathology. Alizarin red staining was used to assess calcium deposits, casein and gelatin zymography were performed to evaluate CAPN and MMP activity, and qPCR was used to evaluate the expression of *Myh, Capn, Atp2a1* and *Atp2a2, Myod1* and *Myog*. We observed the following characteristics in *mdx* muscles: (i) calcium deposits almost exclusively in *mdx* muscles, (ii) lower CAPN1 activity in *mdx* muscles, (iii) higher CAPN2 activity in *mdx* muscles (only at 12 wks), (iv) autolyzed CAPN activity exclusively in *mdx* muscles, (v) lower expression of *Capn1* and higher expression of *Capn2* in *mdx* muscles; (vi) lower expression of *Atp2a1* and *Atp2a2* in *mdx* muscles, (vii) higher MMP (pre pro MMP2, pro MMP2, MMP2 and MMP9) activity in *mdx* muscles, (viii) MMP2 activity exclusively in *mdx* muscles at 12 wks, (ix) MMP9 activity exclusively in *mdx* muscles, (x) higher expression of *Myog* in *mdx* muscles at 12 wks, and (xi) lower expression of *Myh* (*Myh7, Myh2, Myh1, Myh4*) in *mdx* muscles, particularly *Myh*7 and *Myh*2. The collection of our results provides valuable information for a better characterization of *mdx* pathology phenotype.

Key words: *Mdx* mouse, Muscular dystrophy, Calpain, Calcium, Matrix metalloprotease

Offprint requests to: Claudia Mermelstein, Instituto de Ciências Biomédicas, Universidade Federal do Rio de Janeiro, Rio de Janeiro, Brazil. e-mail: mermelstein@ufrj.br or mermelstein@histo.ufrj.br

DOI: 10.14670/HH-18-145

Introduction

Duchenne muscular dystrophy (DMD) is the most severe type of muscular dystrophy, which affects 1 in 3,500 males and is caused by X-linked recessive mutations in the dystrophin gene (Blake et al., 2002; Mercuri and Muntoni, 2013). Dystrophin is a protein with multiple binding sites for proteins from a variety of cellular compartments, including membrane and cytoskeleton. Dystrophin binds to transient receptor potential channel (TRPC) in the sarcolemma, actin and microtubules in the cytoskeleton, and nitric oxide in the sarcoplasm (McGreevy et al., 2015). Nonsense mutations, large deletions or duplications in the dystrophin gene lead to membrane instability and damage causing non-regulated calcium input, concomitant with TRPC deregulation, which contributes to calcium homeostasis impairment, which is further exacerbated by muscle contractile activity (Matsuda et al., 1995; Vandebrouck et al., 2002). Muscles from DMD patients and *mdx* mice contain high concentrations of intracellular calcium, which may contribute to muscle

cell death through the activation of calcium-dependent proteases (Dunn and Radda, 1991; Spencer et al., 1995). Calpains (CAPN) are a ubiquitous and well-conserved family of calcium-dependent cysteine proteases involved in normal skeletal muscle differentiation, but also implicated in several pathological conditions including DMD and autosomal recessive limb-girdle muscular dystrophy type 2A (Zats and Starling, 2005; Buffolo et al., 2015). The mechanisms of CAPN activation are complex but are often involved in response to certain apoptotic signals, oncogenes and tumor-suppressor gene products (Goll et al., 2003).

Calpain 1 (or μ-calpain) and calpain 2 (or m-calpain) are the major isoforms of CAPN and are found ubiquitously in the cytoplasm. Calpain 1 (CAPN1) is half maximally activated by 3-50 μM calcium whereas calpain 2 (CAPN2) requires elevated calcium concentration (400-800 μM) (Goll et al., 2003). CAPN-1 and -2 have similar molecular weight (~80 kDa) and form a heterodimer (~110 kDa) with the small 28 kDa subunit. In the presence of calcium, CAPN suffers an autoproteolytic processing responsible for removal of the small subunit and part of the large subunit with consequent reduction of the molecular weight from ~110 to ~78 kDa (Goll et al., 2003; Campbell and Davies, 2012).

Various structural muscle proteins are potential substrates for CAPN- 1 and -2, including C-protein, desmin, filamin, gelsolin, nebulin, titin, tropomodulin, tropomyosin, troponin I, troponin T, utrophin, vimentin and vinculin (Goll et al., 2003). Specific activities of CAPN-1 and CAPN-2 were found to be significantly elevated in dystrophic muscles from DMD patients (Kar and Pearson, 1976; Reddy et al., 1986) and total CAPN concentration was found elevated in both 4-week and 14-week old *mdx* mice (Spencer et al., 1995). Since dystrophic fibers show increased calcium, and CAPN are activated by calcium, it is important to draw a parallel between CAPN activity and calcium deposition in muscles that are differently affected in DMD pathology. Here, we studied CAPN activity and calcium deposition in different muscles at two different stages of the *mdx* disease (myonecrosis at 4- and regeneration at 12-week old *mdx* mice). We also analyzed the activity of metalloproteases (MMP) and the expression of sarco/endoplasmic reticulum calcium-ATPases *Atp2a1* and *Atp2a2* (SERCAs), myosin heavy chain (*Myh*), myogenic differentiation factors (*Myod1* and *Myog*), aiming to correlate their role in *mdx* disease with the role of calcium and CAPN.

Material and methods

Ethics statement

This study followed the principles of good laboratory animal care and experimentation in compliance with ethical recommendations in the guidelines of the Brazilian College for Animal Experimentation. The study protocol for handling of animals was approved by the Institutional Animal Care Committee (protocol CEUA 00174/09).

Animals

Isogenic male *mdx* (C57BL/10ScSn-Dmdmdx/J) dystrophic and age-matched C57BL/10J (C57) control non-dystrophic mice at 4 and 12 weeks (wks) of age were kept in the animal housing facilities at the Biology Institute at the Fluminense Federal University. Mice were housed in a ventilated rack (Alesco, São Paulo, Brazil) in autoclaved cages and kept at a constant 12 h/12 h light-dark cycle and temperature (24°C) with free access to food and water. Mice were euthanized by cervical dislocation and skeletal muscles with distinct fiber-type characteristics were collected (Moens et al., 1993; Brooks, 1998; Consolino and Brooks, 2004). The following muscles were used in this study: gastrocnemius, triceps-brachii, extensor digitorium longus (EDL) and soleus. Individual muscles were dissected at the ages of 4 and 12 wks corresponding to the height of myonecrosis and regeneration respectively (Grounds et al., 2008). Whole individual muscles were weighted and macerated in lysis buffer (1/10 w/v), for CAPN: [50 mM HEPES, pH 7.6, 150 mM NaCl, 10% (v/v) glycerol, 0.1% (v/v) Triton X-100, 5 mM EDTA, 10 mM 2-mercaptoethanol, 100 µM PMSF, 10 µg/mL leupeptin] (Elce, 2000), for MMP: [100 mM Tris-HCl, pH 7,6, 200 mM NaCl, 100 mM $CaCl_2$, 1% (v/v) Triton X-100], or fixed in formalin and processed into paraffin-embedded blocks (Leite et al., 2010).

Alizarin Red S staining for calcium deposits analysis

Muscles from C57BL10 and *mdx* mice were fixed in 10% neutral buffered formalin and further processed into paraffin-embedded cassettes. Sections of 5 µm in thickness were placed on poly-lysine-coated slides. Muscle sections were stained with Alizarin Red S 2% (ARS) solution for 3 to 5 min and dehydrated in acetone, acetone-xilol (1:1), and xilol, during 20 sec each step and mounted in glycerol (McGee-Russell, 1958). Images of calcium deposits birefringence were observed and acquired under bright-field and polarization microscopy on an Axiovert 100 microscope (Zeiss, Germany). Calcium deposits were quantified under polarized light microcopy, since this contrast-enhancing technique improves the quality of the image obtained with birefringent materials, such as calcium deposits.

Tissue extracts preparation for zymography

Gastrocnemius and triceps brachii muscles from C57BL10 and *mdx* mice were collected and processed individually, while soleus and EDL were processed as a pool of muscles to increase protein quantity. All muscles

were macerated on the same day of dissection on lysis buffer using TissueRuptor (Qiagen, USA) in ice-bath until total dissociation. Muscle extracts were centrifuged for 15 min under 15,000xg at 4°C and the supernatant was recovered and stored until use in aliquots at -20°C. Protein concentration was quantified by Lowry method (Lowry et al., 1951) and 40 μg of protein was loaded in each zymography gel lane.

Casein zymography assay for CAPN activity

Casein gels for analysis of CAPN activity were performed as described previously (Elce, 2000). Briefly, gels consisted of 10% (w/v) polyacrylamide impregnated with casein 10 mg/mL (Sigma), and 5% (w/v) polyacrylamide for stacking gels. Gels were run (Power Pac 200, Bio-Rad, USA) with electrophoresis buffer (25 mM Tris base, 125 mM glycine, 1 mM EDTA, pH 8.0 and 10 mM 2-mercaptoethanol) at 125 Volts. Gels were removed and washed twice for 30 min each with incubation buffer (50 mM Tris-HCl, pH 7.0, 5 mM $CaCl_2$, 10 mM 2-Mercaptoethanol) under gentle swirling. Thereafter gels were transferred to a new incubation buffer and incubated overnight at room temperature under gentle swirling.

Gelatin zymography assay for matrix metalloprotease activity

SDS-PAGE zymography was performed to determine gelatinase activity according to previous description (Heussen and Dowdle, 1980). Briefly, zymogram gels consisted of 7.5% polyacrylamide-SDS gel impregnated with 2 mg/ml type A gelatin from porcine skin (Sigma) and 4% polyacrylamide-SDS for stacking gels. Gels were further washed twice for 30 min in 2.5% Triton X-100 solution, and then incubated at 37°C for 24 h in substrate buffer (10 mM Tris-HCl buffer, pH 7.5 with 5 mM $CaCl_2$, 1 µM $ZnCl_2$). Matrix metalloproteases (MMP) are produced and secreted in its zymogenic form, and once in the extracellular matrix space suffers activation through inhibitory pro-peptide removal, which is also responsible for reducing the molecular weight. The MMP electrophoresis is performed in the presence of SDS, during the washing with renaturation buffer (2.5% Triton X-100), the SDS is removed and activates the enzyme without the inhibitory pro-peptide removal, allowing the identification of inactive enzyme activity (Heussen and Dowdle, 1980; Kherif et al., 1999).

Gel staining

CAPN and MMP gels were stained with stain solution [0.25% (w/v) Coomassie blue, 40% (w/v) methanol, 7% (w/v) acetic acid] and washed with destain solution [50% (w/v) methanol, 10% (w/v) acetic acid] until bands were visible. Zymogram bands appeared as white bands in the gels, but images were inverted to black bands to facilitate visualization.

Image acquisition and quantification

Images from zymograms were acquired using the software L-Pix (Loccus-Brazil) and gel bands were quantified by LabImage (Loccus-Brazil) with a background reduction. Quantification of the area occupied by calcium deposits from Alizarin Red S staining was performed using Image J software.

Gene expression

Total RNA was extracted using the TRIzol Reagent (Invitrogen, Carlsbad, USA) and Nucleo Spin RNA® (Macherey Nagel, Düren, DE). Briefly, aqueous phase from initial TRIzol protocol were placed into the Machery Nagel Nucleo Spin RNA column according to downstream manufacturer's protocols. The cDNA synthesis was performed using the High Capacity cDNA Reverse Transcription Kit (Applied Biosystems, CA, USA) according to manufacturer's protocols using 750 ng for soleus and EDL and 1000 ng for gastrocnemius and triceps-brachii of total RNA. Following cDNA synthesis, mRNA expressions were evaluated by qPCR using the HOT FIREPol® Evagreen® qPCR Supermix (Solis Biodyne, Denmark) using the Master Cycler Realplex system (Eppendorf, Germany). Primer pairs' sequences are shown in Table 1. Quantification of

Table 1. List of primers for qPCR.

Gene	Primer sequences	GenBank accession no.
Atp2a1	GGAATGCAGAGAACGCTATCG TCCTTTGCACTGACTTTCGGT	NM_007504.2 XM_006507268.1
Atp2a2	AATCTGACCCAGTGGCTGATG AGAGGGCTGGTAGATGTGTTG	NM_009722.3
Capn1	ATGACAGAGGAGTTAATCACCCC GCCCGAAGCGTTTCATAATCC	NM_001110504
Capn2	GGTCGCATGAGAGAGCCATC CCCCGAGTTTTGCTGGAGTA	NM_009794
Hprt1	GCAGTACAGCCCCAAAATGG AACAAAGTCGGCCTGTATCCAA	NM_013556.2
Myh1	CGGAGTCAGGTGAATACTCACG GAGCATGAGCTAAGGCACTCT	NM_030679.2
Myh2	TGGAGGGTGAGGTAGAGAGTG TTGGATAGATTTGTGTTGGATTG	NM_001039545.2
Myh4	CACCTGGACGATGCTCTCAGA GCTCTTGCTCGGCCACTCT	NM_010855.3
Myh7	ACTGTCAACACTAAGAGGGTCA TTGGATGATTTGATCTTCCAGGG	NM_080728.3
Myod1	GACCTGCGCTTTTTTGAGGACC CAGGCCCACAGCAAGCAGCGAC	NM_010866.2
Myog	TTGCTCAGCTCCCTCAACCAGGA TGCAGATTGTGGGCGTCTGTAGG	NM_031189.2
Rpl0	GGCCCTGCACTCTCGCTTTC TGCCAGGACGCGCTTGT	NM_007475.5

mRNA expression was calculated from the standard curve method and the expression corrected by the geometric mean of the reference genes (for gastrocnemius and triceps-brachii: Rpl0, Hprt1). The best reference gene combinations were chosen according to their Cq values, using the minor variance between the groups. PCR program was as follows: denaturation 12 min 95°C, 40 cycles of 15 sec 95°C, 30 sec 60°C, 30 sec 72°C, following melting program. qPCR quality and genomic DNA contamination was checked using intron-spanning primers, reverse transcriptase-negative samples from cDNA synthesis and melting curve analysis obtained from each reaction.

Statistical analysis

Data were analyzed with the software GraphPad Prism™ 7.0 (GraphPad Software Inc. San Diego, CA, USA), and to access the level of statistical significance we used t-test non-paired and non-parametric Mann-Whitney test. The results were expressed as mean ± standard deviation (SD). A p-value <0.05 was considered statistically significant.

Results

Excessive calcium influx and increased membrane permeability are early changes in DMD muscles (Allen et al., 2016; Bozycki et al., 2018). Therefore, we decided to evaluate the amount of calcium deposition in gastrocnemius and triceps brachii *mdx* muscles using Alizarin staining, which specifically binds calcium and forms birefringent deposits (Fig. 1A). Several calcium deposits were found in both *mdx* muscles (gastrocnemius

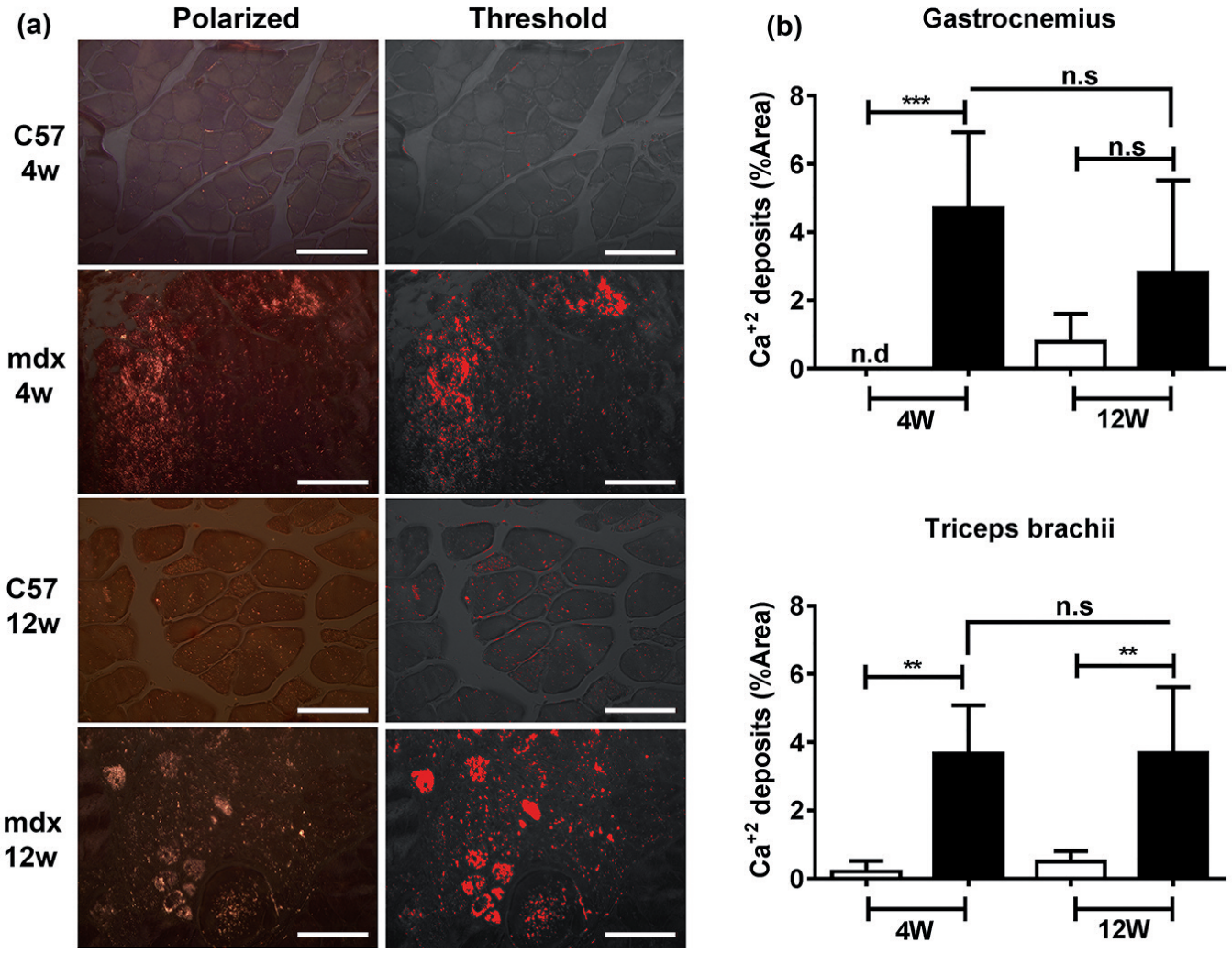

Fig. 1. Calcium deposits are found almost exclusively in *mdx* muscles. Calcium deposits were detected using alizarin staining in gastrocnemius and triceps brachii from C57 control and *mdx* muscles at 4 and 12 wks. One representative image of polarized microscopy from triceps brachii (control and *mdx* at 4 and 12 wks) stained with alizarin is shown in **a**, and the quantification of calcium deposits from both muscles is shown in **b**. **p<0.01, ***p<0.001, n.s. - non-significant, n.d. - non-detected. In **b**, white bar - C57, black bar - mdx. Scale bars: 100 μm.

and triceps brachii) from both ages (4 and 12 wks), while control C57 muscles (gastrocnemius and triceps brachii) from both 4 and 12 wks presented either few or no calcium deposits (Fig. 1B). Interestingly, gastrocnemius and triceps brachii from *mdx* showed no differences between 4 and 12 wks (Fig. 1B).

Since we found increased amounts of calcium deposits in *mdx* muscles compared to control C57 muscles, we decided to analyze whether the high calcium content was related to the activity of calcium-dependent enzymes, such as CAPN and MMP. For the analysis of CAPN activity we used casein zymography, which allows the analysis of the activities of CAPN 1 and 2, as well as CAPN autolyzed forms. Zymogram gels showed 3 distinguishable bands in *mdx* muscle samples: CAPN1, CAPN2 and autolyzed CAPN2 (Fig. 2A), according to previous description (Pomponio et al., 2008). Quantification of zymogram bands showed that CAPN1 activity decreased in all *mdx* muscles (gastrocnemius, triceps brachii, soleus and EDL) at both ages (4 and 12 wks), when compared to age-matched C57 control muscles (Fig. 2B-C). No differences at 4 wks were found in CAPN2 activity in gastrocnemius and triceps brachii, whereas CAPN2 activity was found elevated in soleus and decreased in EDL, all compared to control at 4 wks (Fig. 2A). Interestingly, CAPN2 activity was found elevated at 12 wks in gastrocnemius, soleus and EDL, compared to control at 12 wks. Triceps

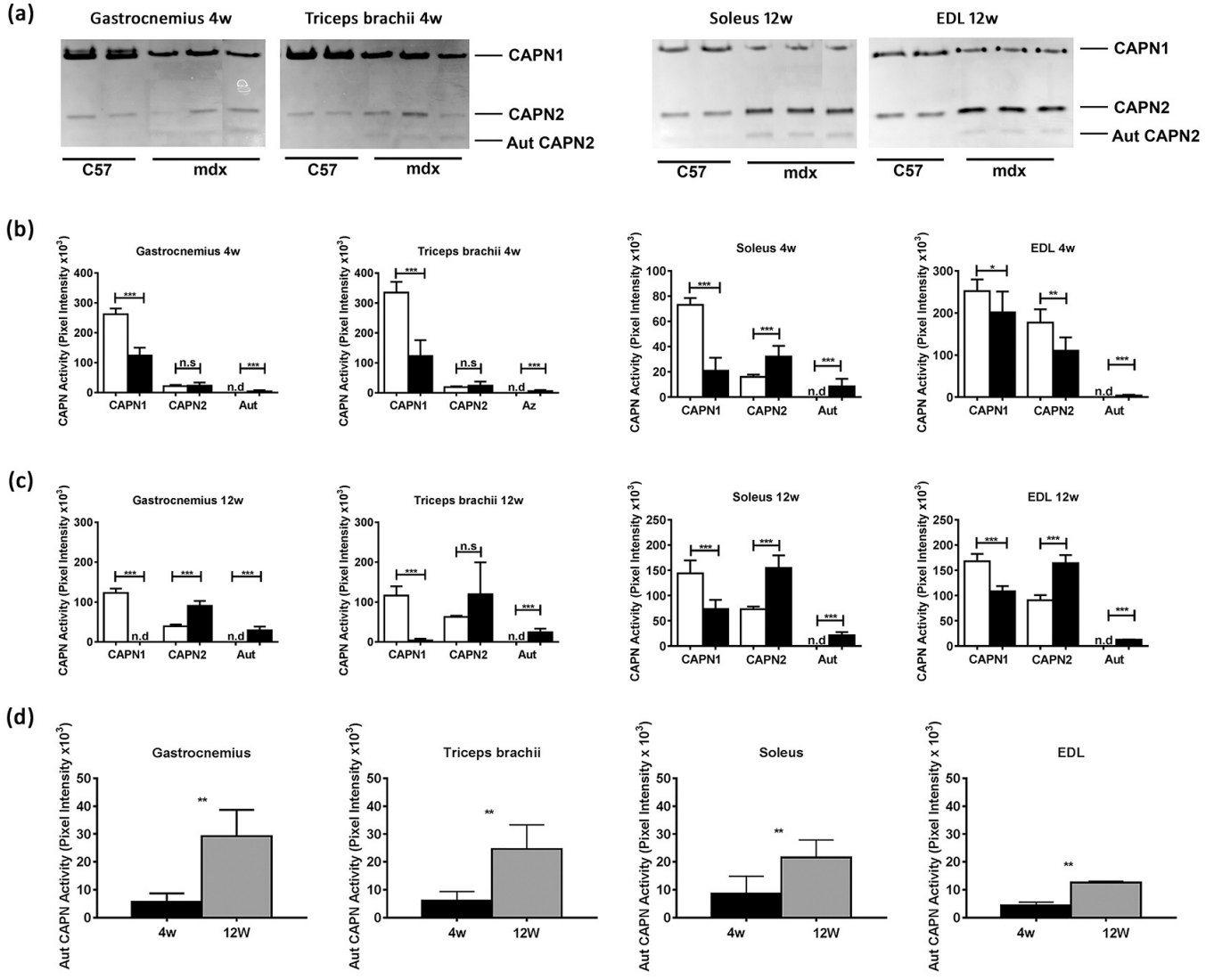

Fig. 2. Calpain activity in *mdx* muscles. **a.** Casein gel zymograms evidencing CAPN1, CAPN2 and autolyzed CAPN in C57 control and *mdx* muscles at 4 and 12 wks (one representative image of each condition is shown). **b.** Quantification of CAPN activity at 4 wks. **c.** Quantification of CAPN at 12 wks. **d.** Quantification of autolyzed CAPN. *p<0.05, **p<0.01, ***p<0.001, n.s. - non-significant, n.d. - non-detected, aut - autolyzed. In **b-c**, white bar - C57, black bar - *mdx*; In **d**, black bar - *mdx* at 4 wks, grey bar - *mdx* at 12 wks.

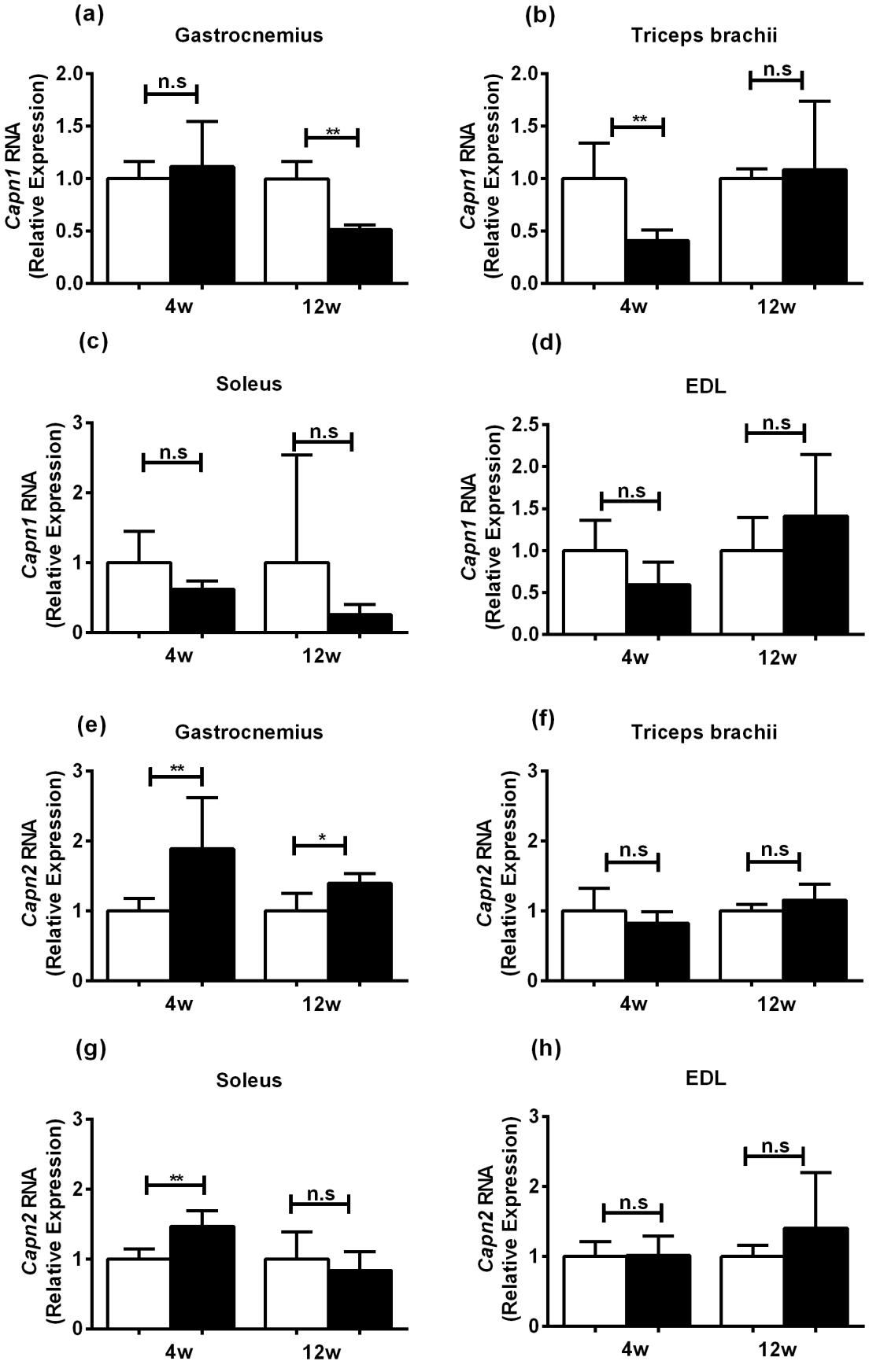

Fig. 3. CAPN gene expression in *mdx* muscles. Relative expression of *Capn1* and *Capn2* genes. **a-d.** *Capn1* gene expression. **e-h.** *Capn2* gene expression. *p<0.05, **p<0.01, n.s. - non-significant. White bar - C57, black bar - *mdx*.

brachii was the only *mdx* muscle at 12 wks that presented no differences compared to control at 12 wks (Fig. 2C). Autolyzed CAPN2, the fully activated form of CAPN2, was only detected in *mdx* muscles (gastrocnemius, triceps brachii, soleus and EDL) at both ages (Fig. 2B,C). We also observed that the amount of autolyzed CAPN2 varies between *mdx* muscles at 4 and 12 wks.

We found differences in the amount of calcium deposits and in the activity of CAPN1, CAPN2 and autolyzed CAPN2 in *mdx* muscles compared to control muscles. Therefore, we decided to analyze the expression of CAPN genes (*Capn1* and *Capn2*) in *mdx* muscles to study if the modulation of CAPN in *mdx* muscles was not only at the enzymatic activity level but also at the transcriptional level. We found a reduced expression of *Capn1* in the gastrocnemius from *mdx* at 12w and in triceps brachii from *mdx* at 4 wks (Fig. 3A,B), while soleus and EDL showed no differences in the expression of *Capn1* either at 4 or 12 weeks (Fig. 3C-D). *Capn2* expression was found elevated in gastrocnemius from *mdx* at both 4 and 12 wks and in soleus from *mdx* at 4 wks (Fig. 3E,G). Triceps brachii and EDL from *mdx* showed no differences in the expression of *Capn2* at both 4 and 12 wks, compared to control (Fig. 3F,H), and soleus from *mdx* showed no differences at 12 wks (Fig. 3G).

Due to elevated calcium deposits found in *mdx* muscles, we decided to analyze the expression of *Atp2a1* and *Atp2a2* (SERCA genes). SERCA are ATPase pumps responsible for transporting calcium from cytosol to endoplasmic reticulum. *Atp2a1* (SERCA1) is expressed exclusively in fast-twitch fibers while *Atp2a2* (SERCA2a) is expressed in slow-twitch fibers (Schiaffino and Reggiani, 2011). qPCR analysis showed a lower expression of *Atp2a1* (SERCA1) and *Atp2a2*

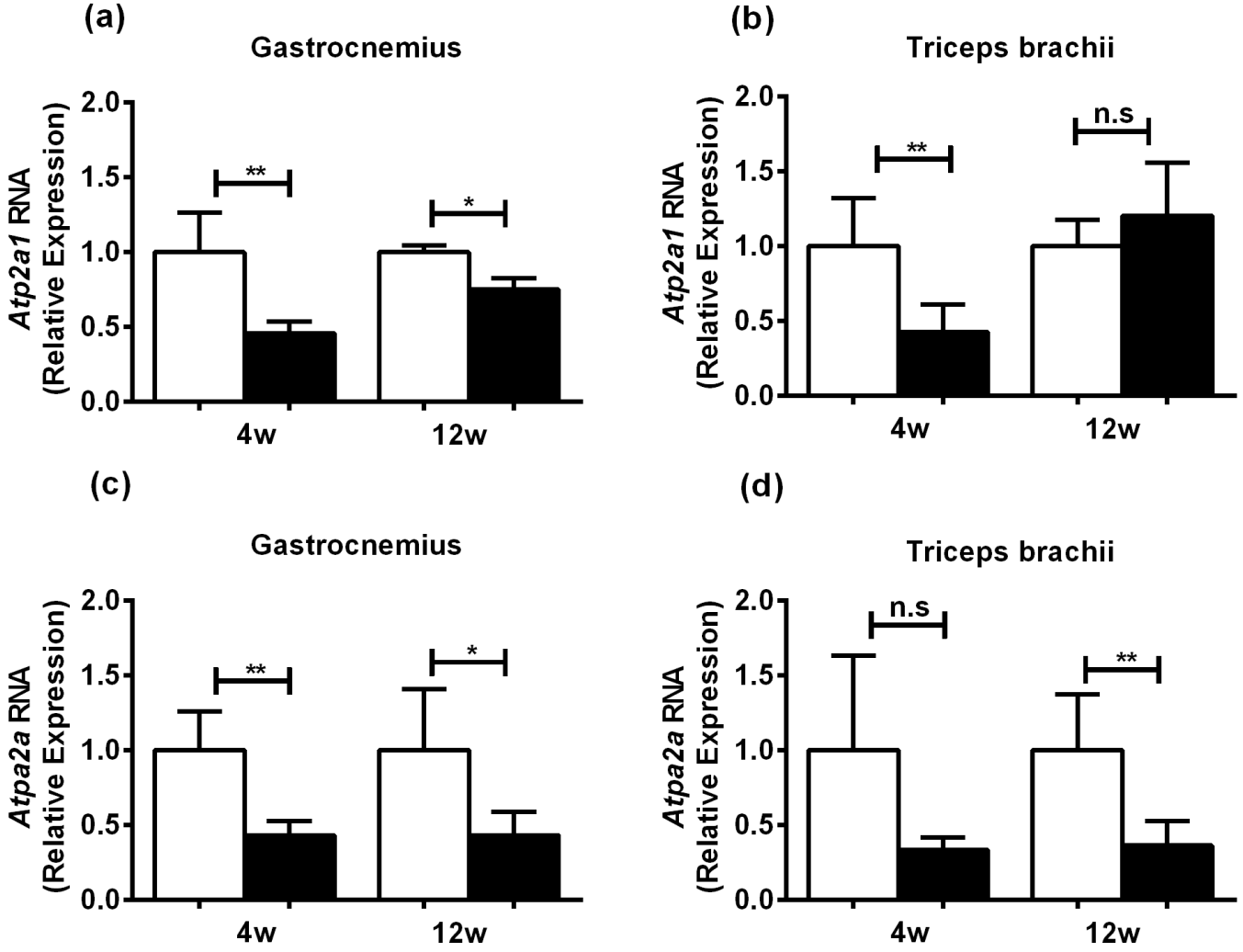

Fig. 4. *Atp2a1* and *Atp2a2* gene expression in *mdx* muscles. Relative expression of *Atp2a1* and *Atp2a2* genes. **a, b.** *Atp2a1* gene expression. **c, d.** *Atp2a2* gene expression. *p<0.05, **p<0.01, n.s. - non-significant. White bar - C57, black bar - *mdx*.

(SERCA2a) in gastrocnemius from *mdx* at 4 and 12 wks when compared to non-dystrophic control (Fig. 4A,C). Triceps brachii from *mdx* showed a lower expression of *Atp2a1* (SERCA1) at 4 wks and of *Atp2a2* (SERCA2a) at 12 wks, compared to C57 control muscles (Fig. 4B,D). The decrease in *Atp2a1* (SERCA1) in *mdx* gastrocnemius was more evident at 4 wks than at 12 wks (Fig. 4A).

We also evaluated the activity of MMP in *mdx* muscles since we found more calcium deposits in *mdx* muscles and MMP are calcium-dependent enzymes. MMP's zymogram gels showed 4 distinguishable bands: the first band at the top of the gel corresponds to MMP-9, and the subsequent bands are pre pro-MMP-2, pro-MMP-2 and active MMP-2, respectively (Fig. 5A). Quantification of the bands evidenced that the zymogenic form of MMP-2 is higher in dystrophic muscles at 4 and 12 wks when compared to C57 control muscles (Fig. 5 b-c). The pre pro-MMP-2 was found higher in *mdx* gastrocnemius, triceps brachii and EDL muscles at both 4 and 12 wks, but not in the soleus (Fig. 5B). In addition, the pro-MMP-2 was found elevated in all *mdx* muscles at both ages (Fig. 5C). The active MMP-2 was found almost exclusively in *mdx* muscles (Fig. 5D); and it was detected in lower levels in C57 gastrocnemius, soleus and EDL at 4 wks (but not in

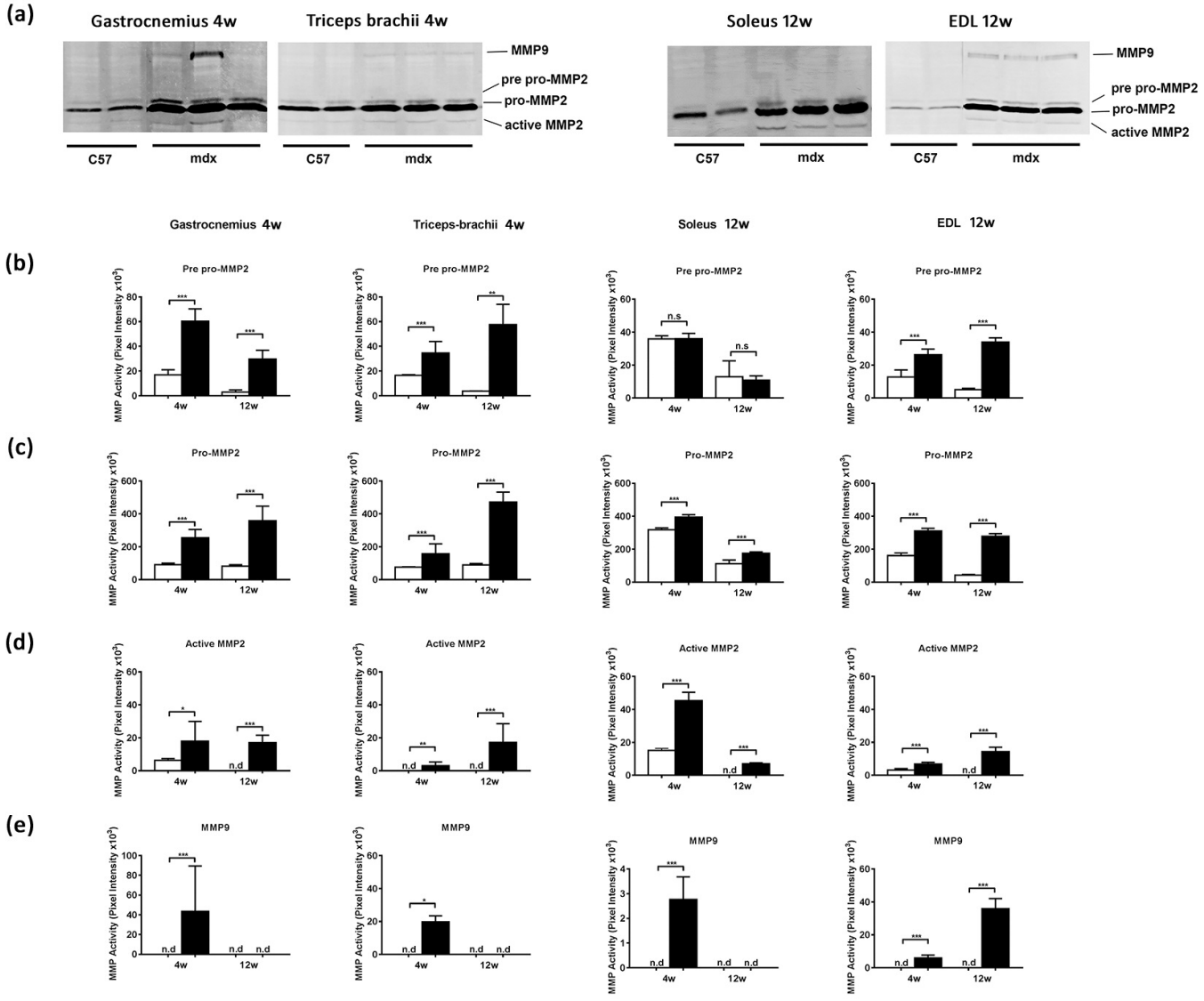

Fig. 5. MMP activity in *mdx* muscles. **a.** Gelatin gel zymogram evidencing MMP9, pre pro-MMP2, pro-MMP2 and MMP2 in C57 and *mdx* muscles at 4 and 12 wks (one representative image of each condition is shown). **b.** Quantification of pre pro-MMP2 activity. **c.** Quantification of pro-MMP2 activity. **d.** Quantification MMP2 activity. **e.** Quantification of MMP9 activity. *p<0.05, * p<0.01, ***p<0.001, n.s. - non-significant, n.d. - non-detected. White bar - C57, black bar - *mdx*.

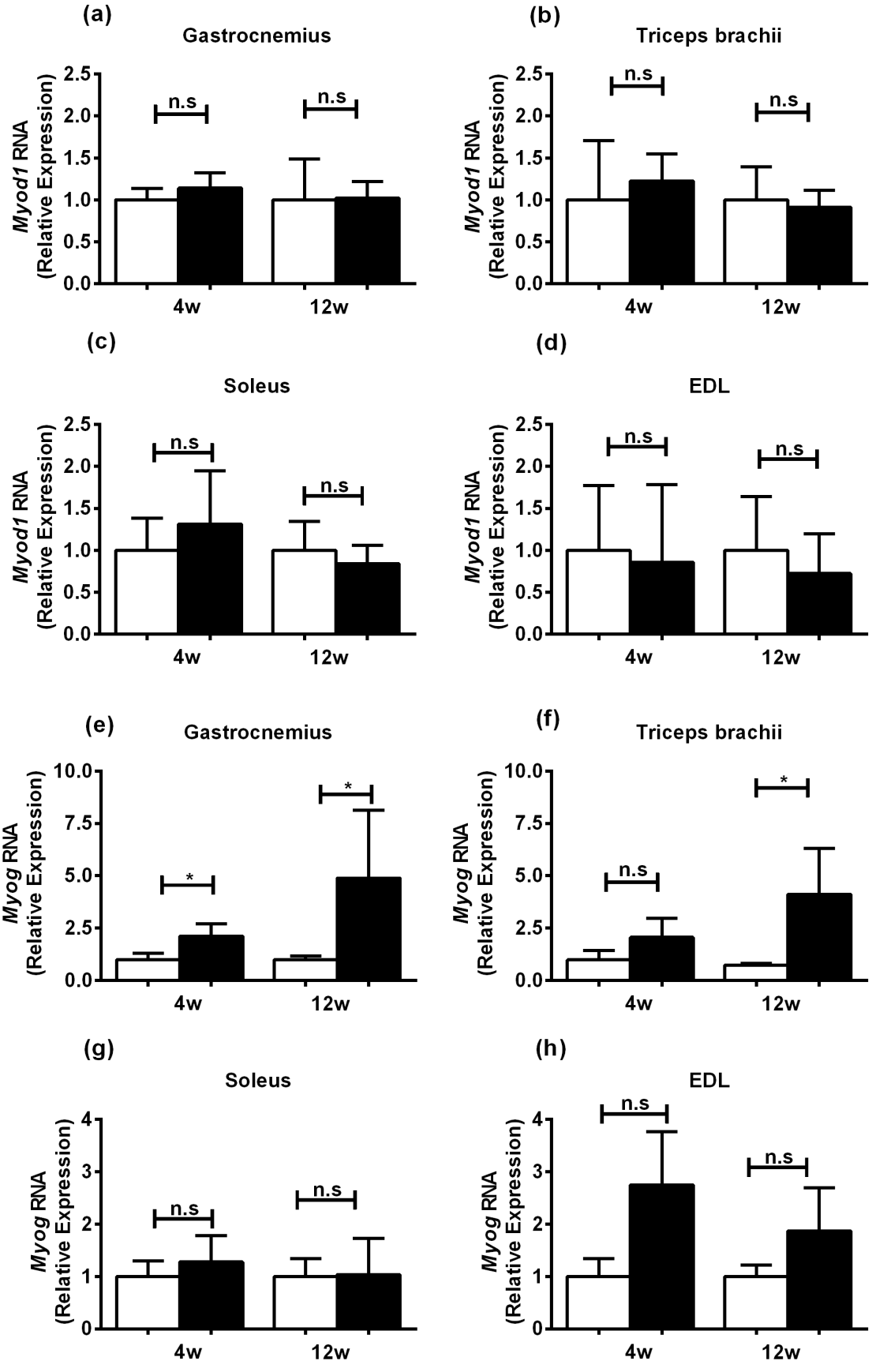

Fig. 6. *MyoD1* and *Myog* gene expression in *mdx* muscles. Relative expression of *MyoD1* and *Myog* genes. **a-d.** *MyoD1* gene expression. **e-h.** *Myog* gene expression. *p<0.05, n.s. - non-significant. White bar - C57, black bar - *mdx*.

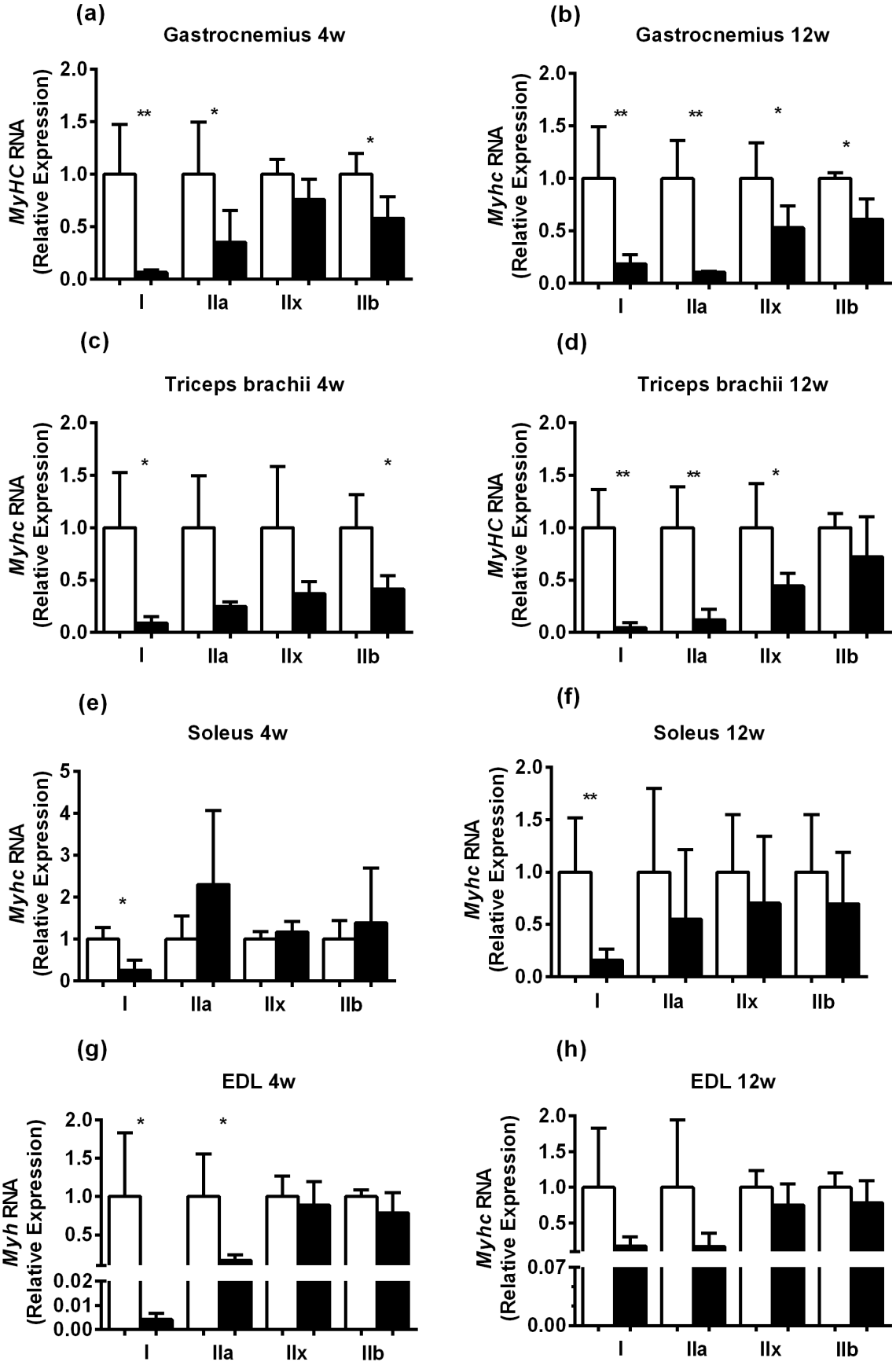

Fig. 7. *Myh* gene expression in *mdx* muscles. Relative expression of *Myh*7, *Myh*2, *Myh*1 and *Myh*4 (type I, IIa, IIx and IIb, respectively). **a, c, e, g.** Mice at 4 wks. **b, d, f, h.** Mice at 12 wks. **a, b.** Gastrocnemius. **c, d.** Triceps brachii. **e, f.** Soleus. **g, h.** EDL. *p<0.05, **p<0.01 (Control versus *mdx*). White bar - C57, black bar - *mdx*.

triceps brachii). MMP-9 was also detected exclusively in *mdx* muscles (gastrocnemius, triceps brachii and soleus) at 4 wks (Fig. 5E), with the only exception of EDL which presented MMP-9 activity at both 4 and 12 wks (Fig. 5E).

To better understand the role of myogenic regulatory factors (MRF) during the *mdx* muscle regeneration process, and to try to correlate it with the observed alterations in calcium, CAPN and MMP activities, we decided to analyze the gene expression levels of *Myod1* and myogenin (*Myog*). MRFs are differentially expressed during different stages of muscle differentiation and we intended to study if their expressions were altered in different *mdx* muscles and/or in different stages of *mdx* muscle disease. *Myod1* expression in all *mdx* muscles (gastrocnemius, triceps brachii, EDL and soleus) and at both ages (at 4 and 12 wks) showed no differences when compared to age-matched C57 control (Fig. 6A-D). An increased expression of *Myog* was found in *mdx* gastrocnemius at both 4 and 12 wks and in *mdx* triceps brachii at 12 wks, compared to C57 control muscles (Fig. 6E-F). Interestingly, *mdx* gastrocnemius and triceps brachii at 12 wks showed more remarkable increases in *Myog* expression than these same *mdx* muscles at 4 wks (Fig. 6E-F). However, soleus and EDL from *mdx* at both 4 and 12 wks showed no differences in *Myog* expression compared to control (Fig. 6G-H).

Muscle fiber types differ in their pattern of expression of myosin heavy chain genes (*Myh*). Therefore, we also evaluated the expression of *Myh* in control and *mdx* muscles to try to correlate different fiber types with the alterations in CAPN and MMP activities observed in our study. There are four *Myh* genes (*Myh7*, *Myh2*, *Myh1*, *Myh4*), which are related to Myh I, IIa, IIx and IIb, respectively. Gastrocnemius and triceps brachii from *mdx* at both ages evidenced a reduced expression of all *Myh*, with a tendency for expressing the fast Myh IIx and IIb coded by *Myh1* and *Myh4* (Fig. 7A-D) and showing lower expression of the slow *Myh7* (type I) and the fast-oxidative *Myh2* (type IIa). Soleus from *mdx* at both ages presented lower levels of *Myh7* (fiber type I) and no significant changes in the expression of other Myh isoforms (Fig. 7E-F). *Mdx* EDL presented an evident reduction in the expression of *Myh7* and *Myh2* (type I and type IIa fibers) at 4 wks, but not at 12 wks (Fig. 7G-H). Interestingly, all *mdx* muscles presented a much lower *Myh7* expression (fiber type I) at both ages.

Discussion

In this study we evaluated calcium deposits, activity of calcium-dependent proteins (CAPN and MMP) and expression of muscle-related genes (CAPN, SERCA, MRF and *Myh*) in distinct skeletal muscles (gastrocnemius, triceps-brachii, soleus and EDL) from *mdx* mice, at two phases of the muscular disease (4 and 12 wks).

Calcium deposits were found almost exclusively in *mdx* dystrophic muscles at both 4 and 12 wks and were not detected in control C57 muscles. Wada and colleagues also described an increase in calcium deposits in tibialis anterior muscle from *mdx* mice (Wada et al., 2014). Recently, our group showed that *mdx* soleus and *mdx* EDL muscles showed calcium deposits, while no deposits were found in control C57 muscles (Gaglianone et al., 2019). We also showed that *mdx* EDL display more calcium deposits than *mdx* soleus (Gaglianone et al., 2019). Interestingly, EDL showed the highest amounts of calcium deposits among all *mdx* muscles tested (gastrocnemius, triceps brachii, soleus and EDL) in both studies (Gaglianone et al., 2019 and the present work). This could be due to contraction-induced membrane lesions (Allen and Whitehead, 2011), which are more susceptible in fast-twitch muscles (such as EDL). In our recent paper we also described that *mdx* EDL and soleus presented more calcium deposits at 12 wks than 4 wks (Gaglianone et al., 2019). Remarkably, here we show that gastrocnemius and triceps brachii display no differences in the amount of calcium deposits between 4 and 12 wks. Further studies are needed to understand why heterogeneous muscles (such as gastrocnemius and triceps brachii) from *mdx* are less susceptible to the accumulation of calcium deposits.

Here we found alterations in CAPN activity in *mdx* muscles. Our results showed that CAPN1 activity is lower in *mdx* muscles, CAPN2 activity is higher in *mdx* muscles at 12 wks and autolyzed CAPN activity was found exclusively in *mdx* muscles. CAPN are activated by calcium. Calpain 1 (CAPN1) is half maximally activated by 3-50 μM calcium whereas calpain 2 (CAPN2) requires elevated calcium concentration (400-800 μM) (Goll et al., 2003). Thus, CAPN2 could be more activated in *mdx* muscles than CAPN1 because more calcium deposits were found in *mdx* muscles at 12 wks. Interestingly, it has been shown that CAPN1 is responsible for repairing small membrane damages, while CAPN2 is required for more extensive damage repair (Mellgren et al., 2009). We found the autolyzed form of CAPN2 exclusively in dystrophic muscles, in accordance with earlier studies (Spencer et al., 1995).

We also analyzed the activity of MMP in *mdx* muscles. We found that the activity of all MMP analyzed (pre pro MMP-2, pro MMP-2, MMP-2 and MMP-9) was increased in *mdx* muscles. Furthermore, MMP2 activity was found exclusively in *mdx* muscles at 12 wks and MMP-9 activity was found exclusively in *mdx* muscles, compared to C57 muscles. These data show that muscles from the *mdx* mice have increased activity of MMP compared to muscles from C57 control. The increase in MMP activity could be related to the intense cycles of tissue repair and remodeling that occur continuously in *mdx* muscles. MMP-2 is described as essential for growth of regenerated muscle fibers through VEGF-associated angiogenesis in the dystrophin-deficient

skeletal muscle (Miyazaki et al., 2011), which is in agreement with our data showing the increased activity of MMP2 in *mdx* muscles at 12 wks (the regeneration phase of *mdx* muscle disease).

In our study, we found MMP-9 activity exclusively in *mdx* muscles, but with varied levels of activation among different muscle types. MMP-9 activity was found almost exclusively in *mdx* muscles at 4 wks, except for *mdx* EDL which presented increased MMP-9 activity at 12 wks. The higher MMP-9 activity in *mdx* EDL at 12 wks (the muscle regeneration phase of *mdx*) could be explained by the fact that fast-twitch muscles are more susceptible to injury and MMP-9 activity could be involved in tissue remodeling. Previous studies from different groups have shown that the amount and activity of MMP-9 are increased in skeletal muscles of animal models of DMD and in muscle biopsies of patients with DMD, and this increase correlates with the severity of disease progression (Kherif et al., 1999; Hindi et al., 2013). How *mdx* muscles can efficiently regenerate despite high amounts and activity of MMP-9, described as deleterious for muscle regeneration, is still not clear and more studies are needed to clarify the ambiguous role of MMP-9 during the remodeling and regeneration of *mdx* muscles.

We also analyzed in the four types of *mdx* muscles the expression of two myogenic regulating factors, *Myod1* and myogenin (*Myog*), which are involved in muscle cell remodeling. No differences were found in the expression of *MyoD1* between *mdx* and C57 control muscles, while *Myog* expression was higher only in *mdx* gastrocnemius and triceps brachii. The higher expression of *Myog* in dystrophic muscles could be caused by activation and differentiation of satellite cells to form new myofibers during muscle regeneration in the *mdx* muscles at 12 wks. Higher (5 times) *Myog* transcript levels in *mdx* mice in hindlimb muscles has been reported previously and the authors suggest that this increase is expected given that *mdx* mice continuously regenerate their damaged muscle (Meadows et al., 2011). We found that *Myog* transcript levels in triceps brachii from *mdx* mice at 12 wks were 4 times higher than C57 control muscle.

We observed a decreased expression of *Atp2a1* (SERCA1) and *Atp2a2* (SERCA2a) in *mdx* gastrocnemius and triceps brachii. In agreement with these data, we have recently reported that *Atp2a1* in *mdx* EDL and *Atp2a2* in *mdx* soleus were significantly lower than control C57 muscles (Gaglianone et al., 2019). In our previous study, we have also shown that *mdx* soleus presented no differences (compared to control C57 muscles) in the expression of *Atp2a1* at both 4 and 12 wks, while a decrease (compared to control C57 muscles) in the expression of *Atp2a2* at both 4 and 12 wks was found in soleus (Gaglianone et al., 2019). We also showed that EDL presented lower expression of *Atp2a1*, compared to control C57 muscle, at 4 wks; and increased expression of *Atp2a2* at 12 wks (Gaglianone et al., 2019). SERCAs are involved in calcium removal from cytosol to the sarcoplasmic reticulum. The higher calcium found in *mdx* muscles could be inhibiting the expression of SERCAs, as previously reported (Zhao et al., 2012). One possible hypothesis could be that calcium deposits inhibit the expression of calcium-related proteins (including Ca^{2+}-ATPases and calsequestrin-like proteins) in *mdx* fibers (Kargacin and Kargacin, 1996; Culligan et al., 2002; Zhao et al., 2012), leading to a worse ability to handle calcium changes and thus enhancing myonecrosis.

The properties of a muscle fiber type can have an impact in the phenotype of a muscle disease and changes in Myh isoforms can have effects on DMD physiopathology (Beedle, 2016). Fiber type remodeling is recurrent in the dystrophic muscle, where an increase in type I fibers was shown in a variety of muscles (Coirault et al., 1999; Spassov et al., 2010; Camerino et al., 2014). We evaluated mRNA levels of all four isoforms of Myh (I, IIa, IIb and IIx) at the peak of myonecrosis and the peak of regeneration of dystrophic *mdx* muscles. The results evidenced that most of the dystrophic muscles presented a reduction in the expression of all Myh isoforms (I, IIa, IIb and IIx) when compared to non-dystrophic C57 control muscles. However, the comparative expression of each isoform was found quite variable in each muscle type. The change in the expression of Myh isoforms could be related to low mitochondrial activity. Myh consumes high amounts of ATP in muscle fibers, and therefore are highly affected by energy supply (Vallejo-Illarramendi et al., 2014). Our group has recently shown that dystrophic muscle fibers present reduced mitochondrial activity (Gaglianone et al., 2019).

Remarkably, our study found several characteristics to be specific to *mdx* muscles at 12 wks (Compared to control at 12 wks): CAPN2 activity was increased at 12 wks, MMP-2 activity was found exclusively at 12 weeks, and expression of myogenin (*Myog*) was increased at 12 wks. This phase of the *mdx* muscular pathology, 12 wks, is when regeneration of muscle tissue is at its peak (Grounds et al., 2008), and therefore, our results reinforce a role for CAPN2, MMP-2 and myogenin in the remodeling of *mdx* muscle. In conclusion, in the present study we found a parallel between increased calcium deposits and alterations in the expression and activity of calcium-related enzymes (CAPN and MMP) in *mdx* muscles, confirming the important role of calcium in the *mdx* pathology.

Acknowledgements. The authors thank Juliana Lourenço for expert technical assistance. This work was supported by grants from Conselho Nacional de Desenvolvimento Científico e Tecnológico (CNPq), Fundação Carlos Chagas Filho de Apoio à Pesquisa do Estado do Rio de Janeiro (FAPERJ), Coordenação de Aperfeiçoamento de Pessoal de Nível Superior (CAPES). This work is part of RBG's master thesis at the Programa de Pós-Graduação em Ciências Morfológicas (PCM/UFRJ).

Competing Interests Statement. The authors declare that they have no conflicts of interest concerning this article.

References

Allen D.G. and Whitehead N.P. (2011). Duchenne muscular dystrophy-what causes the increased membrane permeability in skeletal muscle? Int. J. Biochem. Cell Biol. 43, 290-294.

Allen D.G., Whitehead N.P. and Froehner S.C. (2016). Absence of dystrophin disrupts skeletal muscle signaling: roles of Ca^{2+}, reactive oxygen species, and nitric oxide in the development of muscular dystrophy. Physiol. Rev. 96, 253-305.

Beedle A.M. (2016). Distribution of myosin heavy chain isoforms in muscular dystrophy: insights into disease pathology. Musculoskelet. Regen. 2, e1365.

Blake D.J., Weir A., Newey S.E. and Davies K.E. (2002). Function and genetics of dystrophin and dystrophin-related proteins in muscle. Physiol. Rev. 82, 291-329.

Bozycki L., Łukasiewicz K., Matryba P. and Pikula S. (2018). Whole-body clearing, staining and screening of calcium deposits in the mdx mouse model of Duchenne muscular dystrophy. Skeletal Muscle 8, 21.

Brooks S.V. (1998). Rapid recovery following contraction-induced injury to in situ skeletal muscles in *mdx* mice. J. Muscle Res. Cell Motil. 19, 179-187.

Buffolo M., Batista Possidonio A.C., Mermelstein C. and Araujo H. (2015). A conserved role for calpains during myoblast fusion. Genesis 53, 417-430.

Camerino G.M., Cannone M., Giustino A. Massari A.M., Capogrosso R.F., Cozzoli A. and De Luca A. (2014). Gene expression in *mdx* mouse muscle in relation to age and exercise: aberrant mechanical-metabolic coupling and implications for pre-clinical studies in Duchenne muscular dystrophy. Human Mol. Genet. 23, 5720-5732.

Campbell R.L. and Davies P.L. (2012). Structure-function relationships in calpains. Biochem. J. 447, 335-351.

Coirault C., Lambert F., Marchand-Adam S., Attal P., Chemla D. and Lecarpentier Y. (1999). Myosin molecular motor dysfunction in dystrophic mouse diaphragm. Am. J. Physiol. Cell Physiol. 277, C1170-C1176.

Consolino C.M. and Brooks S.V. (2004). Susceptibility to sarcomere injury induced by single stretches of maximally activated muscles of *mdx* mice. J. App. Physiol. 96, 633-638.

Culligan K., Banville N., Dowling P. and Ohlendieck K. (2002). Drastic reduction of calsequestrin-like proteins and impaired calcium binding in dystrophic *mdx* muscle. J. Appl. Physiol. 92, 435-445.

Dunn J. and Radda G. (1991). Total ion content of skeletal and cardiac muscle in the mdx mouse dystrophy: Ca^{2+} is elevated at all ages. J. Neurol. Sci. 103, 226-231.

Elce J.S. (2000). Calpain methods and protocols. Vol 144. Springer Science & Business Media, New York, USA.

Gaglianone R.B., Santos A.T., Bloise F.F., Ortiga-Carvalho T.M., Costa M.L., Quirico-Santos T., Silva W.S. and Mermelstein C. (2019). Reduced mitochondrial respiration and increased calcium deposits in the EDL muscle, but not in soleus, from 12-week-old dystrophic *mdx* mice. Sci. Rep. 9, 1986.

Goll D.E., Thompson V.F., Li H., Wei W. and Cong J. (2003). The calpain system. Physiol. Rev. 83, 731-801.

Grounds M.D., Radley H.G., Lynch G.S. Nagaraju K. and De Luca A. (2008). Towards developing standard operating procedures for pre-clinical testing in the *mdx* mouse model of Duchenne muscular dystrophy. Neurobiol. Dis. 31, 1-19.

Heussen C. and Dowdle E.B. (1980). Electrophoretic analysis of plasminogen activators in polyacrylamide gels containing sodium dodecyl sulfate and copolymerized substrates. Anal. Biochem. 102, 196-202.

Hindi S.M., Shin J., Ogura Y. Li H. and Kumar A. (2013). Matrix metalloproteinase-9 inhibition improves proliferation and engraftment of myogenic cells in dystrophic muscle of *mdx* mice. PLoS One 8, e72121.

Kargacin M.E. and Kargacin G.J. (1996). The sarcoplasmic reticulum calcium pump is functionally altered in dystrophic muscle. Biochim. Biophys. Acta 1290, 4-8.

Kar N.C. and Pearson C.M. (1976). A calcium-activated neutral protease in normal and dystrophic human muscle. Clin. Chim. Acta 73, 293-297.

Kherif S., Lafuma C., Dehaupas M., Lachkar S., Fournier J.G., Verdière-Sahuqué M., Fardeau M. and Alameddine H.S. (1999). Expression of matrix metalloproteinases 2 and 9 in regenerating skeletal muscle: a study in experimentally injured and *mdx* muscles. Dev. Biol. 205, 158-170.

Leite P.E.C., Lagrota-Candido J., Moraes L., D'Elia L., Pinheiro D.F., da Silva R.F., Yamasaki E.M. and Quirico-Santos T. (2010). Nicotinic acetylcholine receptor activation reduces skeletal muscle inflammation of *mdx* mice. J. Neuroimmunol. 227, 44-51.

Lowry O.H., Rosebrough N.J., Farr A.L. and Randall R.J. (1951). Protein measurement with the Folin phenol reagent. J. Biol. Chem. 193, 265-275.

Matsuda R., Nishikawa A. and Tanaka H. (1995). Visualization of dystrophic muscle fibers in *mdx* mouse by vital staining with Evans blue: evidence of apoptosis in dystrophin-deficient muscle. J. Biochem. 118, 959-963.

McGee-Russell S. (1958). Histochemical methods for calcium. J. Histochem. Cytochem. 6, 22-42.

McGreevy J.W., Hakim C.H., McIntosh M.A. and Duan D. (2015). Animal models of Duchenne muscular dystrophy: from basic mechanisms to gene therapy. Dis. Models Mech. 8, 195-213.

Meadows E., Flynn J.M. and Klein W.H. (2011). Myogenin regulates exercise capacity but is dispensable for skeletal muscle regeneration in adult *mdx* mice. PLoS One 6, e16184.

Mellgren R.L., Miyake K., Kramerova I., Spencer M.J., Bourg N., Bartoli M., Richard I., Greer P.A. and McNeil P.L. (2009). Calcium-dependent plasma membrane repair requires m- or μ-calpain, but not calpain-3, the proteasome, or caspases. Biochim. Biophys. Acta 1793, 1886-1893.

Mercuri E. and Muntoni F. (2013). Muscular dystrophies. Lancet 381, 845-860.

Moens P., Baatsen P. and Maréchal G. (1993). Increased susceptibility of EDL muscles from *mdx* mice to damage induced by contractions with stretch. J. Muscle Res. Cell Motil. 14, 446-451.

Miyazaki D., Nakamura A., Fukushima K. Yoshida K., Takeda S. and Ikeda S. (2011). Matrix metalloproteinase-2 ablation in dystrophin-deficient mdx muscle reduces angiogenesis resulting in impaired growth of regenerated muscle fibers. Hum. Mol. Genet. 20, 1787-1799.

Pomponio L., Lametsch R., Karlsson A.H., Costa L.N., Grossi A. and Ertbjerg P. (2008). Evidence for post-mortem m-calpain autolysis in porcine muscle. Meat Sci. 80, 761-764.

Reddy P.A., Anandavalli T. and Anandaraj M. (1986). Calcium activated neutral proteases (milli- and micro-CANP) and endogenous CANP inhibitor of muscle in Duchenne muscular dystrophy (DMD). Clin. Chim. Acta 160, 281-288.

Schiaffino S. and Reggiani C. (2011). Fiber types in mammalian skeletal muscles. Physiol. Rev. 91, 1447-1531.

Spassov A., Gredes T., Gedrange T., Lucke S., Morgenstern S., Pavlovic D. and Kunert-Keil C. (2010). Differential expression of myosin heavy chain isoforms in the masticatory muscles of dystrophin-deficient mice. Eur. J. Orthod. 33, 613-619.

Spencer M.J., Croall D.E. and Tidball J.G. (1995). Calpains are activated in necrotic fibers from *mdx* dystrophic mice. J. Biol. Chem. 270, 10909-10914.

Vallejo-Illarramendi A., Toral-Ojeda I., Aldanondo G. and López de Munain A. (2014). Dysregulation of calcium homeostasis in muscular dystrophies. Exp. Rev. Mol. Med. 16, e16.

Vandebrouck C., Martin D., Colson-Van Schoor M., Debaix H. and Gailly P. (2002). Involvement of TRPC in the abnormal calcium influx observed in dystrophic (mdx) mouse skeletal muscle fibers. J. Cell Biol. 158, 1089-1096.

Wada E., Yoshida M., Kojima Y. Nonaka I., Ohashi K., Nagata Y., Shiozuka M., Date M., Higashi T., Nishino I. and Matsuda R. (2014). Dietary phosphorus overload aggravates the phenotype of the dystrophin-deficient mdx mouse. Am. J. Pathol. 184, 3094-3104.

Zatz M. and Starling A. (2005). Calpains and disease. N. Eng. J. Med. 352, 2413-2423.

Zhao X., Moloughney J.G., Zhang S., Komazaki S. and Weisleder N. (2012). Orai1 mediates exacerbated Ca^{2+} entry in dystrophic skeletal muscle. PLoS One 7, e49862.

Accepted July 5, 2019